Draft version December 18, 2016
Typeset using LaTeX **twocolumn** style in AASTeX61

THE FRB 121102OBSERVING CAMPAIGN: MULTI-TELESCOPE RADIO BURST AND IMPLICATIONS FOR THE FRB POPULATION

C. J. Law,[1] G. C. Bower,[2] S. Burke-Spolaor,[3,4,5] B. J. Butler,[3] S. Chatterjee,[6] J. M. Cordes,[6] P. Demorest,[3] J. W. T. Hessels,[7,8] R. Fender,[9] T. J. W. Lazio,[10] D. Michilli,[8] M. A. McLaughlin,[4,5] K. Mooley,[9] M. Rupen,[11] L. G. Spitler,[12] P. Scholz,[11] A. Seymour,[13,14] and R. S. Wharton[6]

[1] *Dept of Astronomy and Radio Astronomy Lab, University of California, Berkeley, CA 94720, USA*
[2] *Academia Sinica Institute of Astronomy and Astrophysics, 645 N. A'ohoku Place, Hilo, HI 96720, USA*
[3] *National Radio Astronomy Observatory, Socorro, NM 87801, USA*
[4] *Department of Physics and Astronomy, West Virginia University, Morgantown, WV 26506, USA*
[5] *Center for Gravitational Waves and Cosmology, West Virginia University, Chestnut Ridge Research Building, Morgantown, WV 26505*
[6] *Cornell Center for Astrophysics and Planetary Science and Department of Astronomy, Cornell University, Ithaca, NY 14853, USA*
[7] *ASTRON, Netherlands Institute for Radio Astronomy, Postbus 2, 7990 AA, Dwingeloo, The Netherlands*
[8] *Anton Pannekoek Institute for Astronomy, University of Amsterdam, Science Park 904, 1098 XH Amsterdam, The Netherlands*
[9] *University of Oxford, UK*
[10] *Jet Propulsion Laboratory, California Institute of Technology, Pasadena, CA 91109, USA*
[11] *National Research Council of Canada, Herzberg Astronomy and Astrophysics, Dominion Radio Astrophysical Observatory, P.O. Box 248, Penticton, BC V2A 6J9, Canada*
[12] *Max-Planck-Institut für Radioastronomie, Auf dem Hügel 69, D-53121 Bonn, Germany*
[13] *Arecibo Observatory, HC3 Box 53995, Arecibo, PR 00612, USA*
[14] *Max-Planck-Institut für Radioastronomie, Auf dem Hügel 69, Bonn, D-53121, Germany*

ABSTRACT

The millisecond radio transients known as Fast Radio Bursts have recently emerged as a mysterious, new class of astrophysical transient. The discovery of repeating bursts from FRB 121102 has shown that at least some FRBs are not cataclysmic and opened potential for studying FRB properties via a homogenous sample of bursts. The recent localization of FRB 121102 with the Very Large Array has helped measure its distance and a host of intrinsic properties. This localization was made with 9 bursts seen by the VLA in coordination the Arecibo, Effelsberg, and AMI-LA observatories. We present a detailed analysis of these bursts, including the first simultaneous detection of an FRB with multiple telescopes. We show that the burst spectra typically have a broad Gaussian shape on the scale of ~ 500 MHz with fine spectral structure consistent with either scintillation or unresolved temporal structure. We present the luminosity distribution and temporal statistics for FRB 121102 and argue that the whole FRB population is adequately described by a single class similar to FRB 121102. We close with thoughts on optimal strategies to make new interferometric localizations of FRBs.

1. INTRODUCTION

Fast Radio Bursts (FRBs) are a new class of millisecond-duration radio transient with a dispersion measure (DM) that implies that they originate outside of our Galaxy. At extragalactic (and potentially cosmological) distances, they are not only unusually luminous, but they provide a new tracer of other galaxies and the intergalactic medium (IGM). In this way, FRBs have opened a whole new playground in astrophysics (e.g., Falcke & Rezzolla 2014; McQuinn 2014; Cordes & Wasserman 2016). However, that potential has been hamstrung by the lack of a definitive association of an FRB to an extragalactic host.

This paper is part of a series that presents the first localization and unambiguous identification of an FRB host (Chatterjee et al 2017; Tendulkar et al 2017; Marcote et al 2017). FRB 121102, also known as the "repeating FRB", was first detected in November 2012 by the Arecibo Observatory (Spitler et al. 2014). In mid 2015, new Arecibo observations revealed a series of bursts at the same DM and sky position demonstrating that FRBs are capable of repetition (Spitler et al. 2016). Beginning in August of 2015, we made the first of nine detections of FRB 121102 with the Very Large Array (Chatterjee et al 2017) and localized it with a precision of $0.1''$. Deep radio and optical observing shows that FRB 121102 is unambiguously associated with a persistent radio and optical source at a redshift of 0.193 (Tendulkar et al 2017; Marcote et al 2017).

FRB 121102 has now been localized four orders of magnitude better than any other FRB and placed at a cosmological distance. Its lookback and luminosity distances are 746 and 972 Mpc (**?**), which are orders of magnitude larger than any other millisecond transient. This shows that FRBs are more luminous than any other millisecond radio transient, have a significant DM contribution from the IGM, and can be used to probe the IGM and their host galaxy. The promise implied by the first reported FRB (Lorimer et al. 2007) is now being realized.

The confirmation of a cosmological distance for FRB 121102 could have wide-ranging implications for the FRB population as a whole. However, it has not been demonstrated that FRB 121102 is representative of the overall FRB population. In fact, the repetition of its bursts is unique among all FRBs (Petroff et al. 2015), so it is natural to ask whether FRB 121102 is representative. An important first step is to demonstrate that the properties of FRB 121102 are consistent with the significant body of facts for the overall population (Macquart & Johnston 2015; Katz 2016). The repeating nature of FRB 121102 provides us with several statistical tests we can use to test this connection.

We can also assume that FRB 121102 is representative and use it to constrain the physical processes at play in the overall FRB population. Although we now know that FRBs are luminous, it is not yet clear what process generates the radio bursts themselves (Katz 2014; Luan & Goldreich 2014; Cordes & Wasserman 2016). The simultaneous FRB 121102 observing campaign with the VLA, Arecibo, Effelsberg, GBT, and AMI-LA gives a more complete picture of the spectral structure of FRB radio emission. FRB repetition also has strong implications for the number of FRB-generating systems in the universe (Connor et al. 2016).

Given that FRBs are now known to be useful probes of the IGM, there is even more motivation to make new detections and localizations. The relatively faint counterpart to FRB 121102 argues that direct localization of the radio burst will continue to be the best way to find optical hosts to measure distances. Our multi-telescope constraints on burst spectra, measurement of host properties, burst rate estimates, and other properties will inform new strategies for finding FRBs.

2. OBSERVATIONS

The data presented here were obtained from multiple programs and telescopes, but the central goal was to interferometrically localize FRB 121102 with the VLA. The observing strategy was to ensure simultaneous observing between the VLA and Arecibo observatories and add other observatories added on a best-effort basis. We coordinated observing between the VLA, Arecibo, Effelsberg, and AMI-LA telescopes, as shown in figure 1. Below, we summarize these observations, with a focus on those conducted simultaneously with VLA burst detections from FRB 121102.

2.1. *VLA*

The FRB 121102 observing campaign started in late 2015 with a 10 hr campaign observed at 1.4 GHz in the compact D configuration. In April through May 2016, we conducted a 40 hr campaign at 3 GHz in the C and CnB configurations in coordination with Arecibo. We concluded with a new, 40 hr, coordinated campaign from August through September 2016 in the B configuration and during the move to the most extended A configuration. In this last campaign, the first 34 hours of VLA observations were made at 3 GHz, while the last 6 hours were observed at 6 GHz. This paper focuses on the data collected at 3 GHz, which includes all nine burst detections.

All VLA fast-sampled data were observed with 5 ms sampling, 256 channels, and dual-circular polarization

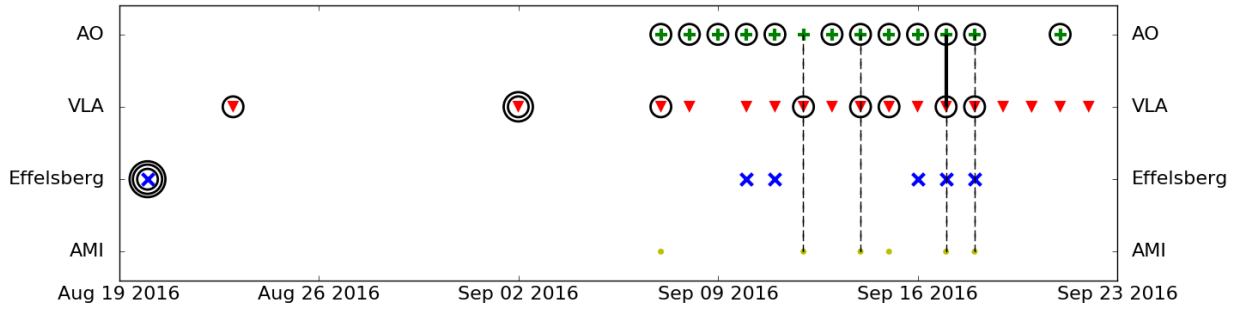

Figure 1. Summary of observing coverage and detections of FRB 121102 during the multi-telescope observing campaign in August and September 2016. Symbols show days with observations and circles highlight observations that detected bursts from FRB 121102. Multiple circles indicate multiple burst detections, except for Arecibo, which typically has multiple detections per observing session (a detailed analysis is left for a future paper). The black dashed lines show the VLA burst detections with simultaneous coverage at other telescopes. The solid black line shows the simultaneous burst detection at VLA and Arecibo.

(Law et al. 2015, as in). To maximize sensitivity, the channel frequency width was set to maintain sensitivity to the known DM of FRB 121102, while maximizing the total bandwidth. The total bandwidth at L (1.4 GHz), S (3 GHz), and C (6 GHz) bands was 256 MHz, 1024 MHz, and 2048 MHz, respectively. The 3 GHz data were recorded data in 8 spectral windows with 32 channels each.

Observations in August and Septmeber were searched by a prototype version of *realfast*[1]. *realfast* is a real-time, fast imaging transient search system. The current, prototype runs on existing, CPU-based hardware of the VLA correlator backend, while the future *realfast* will run on a dedicated GPU cluster. The transient search pipeline software is called *rtpipe*[2] and is mostly written in Python (detail in Law et al. (2015)). Images were formed for each integration at DMs of 0, 546, 556.9, 560, and 565 pc cm^{-3}. Gain calibration is read from the "telcal" system, which uses phase-only calibration on the previous gain calibrator. A flux scale is calculated for each spectral window from an observation on xx (Bryan) and applied to all burst spectra.

Burst detections and localizations were made within hours of data being recorded. The transient search starts when data are recorded, but this prototype of *realfast* is a factor of several times slower than real-time, so we refer to the detection as "quasi real-time". Each image with a pixel higher than 6.4σ is saved in a summary form as a check of data quality. For each image with a pixel higher than 7.4σ, *realfast* generates a more detailed candidate visualization with an image and spectrum. More detailed analysis, including improved calibration and localization, is conducted offline.

Computational notebooks to reproduce the transient detection and localization can be found at `https://github.com/caseyjlaw/FRB121102`. Time cut-out visibility data are available at `https://doi.org/10.7910/DVN/TLDKXG`. Original visibility data are available under VLA program codes 16A-459 and 16A-496 and can be downloaded at `http://archive.nrao.edu`.

2.2. *Arecibo*

copied from the first paper During the joint Arecibo-VLA campaign, Arecibo observed with the L-wide receiver, which has an observational frequency range of 1.15 to 1.73 GHz and a full width at half maximum beam size of 3.3 arcmin. The PUPPI pulsar backend was used to record total intensity spectra with time and frequency resolutions of 10.24 μs and 1.5625 MHz, respectively, and full Stokes polarization information. Each frequency channel was coherently dedispersed to 557 pc cm^{-3}, thereby eliminating intra-channel dispersion smearing. PUPPI covers a total of 800 MHz of bandwidth centred at 1380.78125 MHz, but only $\sim$ 620 MHz of this band is usable due to radio frequency interference and receiver sensitivity roll-off at the band edges.

In total, twelve Arecibo observations had some simultaneous coverage with the VLA. Four of those observations were simultaneous with bursts detected with the VLA and one of those observations detected the same VLA burst. During the first VLA burst with Arecibo coverage (MJD 57643), the PUPPI system failed so data were recorded with xx (Jason?) at C band. No detection was made in that Arecibo data. Overall, there were many more bursts detected at Arecibo than with the VLA and a more detailed analysis of those bursts will be presented in a future paper.

[1] See `http://realfast.io`.
[2] See `https://github.com/caseyjlaw/rtpipe`

2.3. *Effelsberg*

copied from Laura's paper Observations were conducted at an observing frequency of 4.6 to 5.1 GHz. The S60mm receiver has a system equivalent flux density of 18 Jy and a full-width half-max (FWHM) beam size of 2.4′at 4.85 GHz. Pulsar search mode data were recorded with the PFFTS backend. Total intensity spectra were recorded with a time resolution of 65.5 μs and a bandwidth of 500 MHz divided into 128 frequency channels. Note, the inter-channel DM smearing time for 560 pc cm^{-3} is ∼0.2 msec at 4.6 GHz.

Five Effelsberg observations had some simultaneous coverage with the VLA, of which two were simultaneous with VLA bursts. Unfortunately, due to a configuration error, a 100 MHz bandwidth filter centered at 4.85 GHz was in place for both of these sessions. The sensitivity was about two times worse than the nominal value. No burst was detected in either observation.

2.4. *AMI*

We observed FRB 121102with the Arcminute MicroKelvin Imager Large Array (AMI-LA; Zwart et al. 2008) for 3 hours each on four epochs starting at MJDs 57643.3351, 57645.3317, 57648.3352, and 57649.3353. Observations were made with the new digital correlator having 4096 channels across a 5 GHz bandwidth between 13–18 GHz with a 1s dump time. The phase calibrator, J0518+3306, was observed every 12 minutes for about 1.5 minutes. The AMI-LA data were binned to eight 0.625 GHz channels and processed (RFI excision and calibration) with a fully-automated pipeline, AMI-REDUCE (e.g., Perrott et al. 2013). Daily measurements of 3C48 and 3C286 were used for the absolute flux calibration, which is good to about 10%.

We inspected the calibrated visibilities, and did not find any signal above 20 mJy in the 1s samples at and in the vicinity of the detected bursts. Concatenating and imaging the 12 hours of calibrated data with the CASA tasks *concat* and *clean* also does not yield any significant detection at the FRB location. Although the statistical 3sigma upper limit is 60 uJy, extended mJy-level sources in the field cause sidelobe confusion (the AMI-LA angular resolution is ∼30 arcsec), and the actual upper limit is larger. We introduced artificial point sources at the FRB location using the CASA *sm* tool, and found that these sources can be recovered as long as their peak flux densities are more than ∼100 uJy. Hence, we place an upper limit of 100±10 uJy on any quiescent or possible radio "afterglow" (on ∼days timescale) signal from the FRB. This limit is close to the flux density measured by the VLA (Chatterjee et al 2017).

3. RESULTS

3.1. *Multi-Telescope Burst Spectrum*

Four of the VLA bursts were observed simultaneously with Arecibo and AMI-LA (Figure 1). Of these, the burst on 57648 was detected by Arecibo at the same time (after correcting for the known DM of FRB 121102). The Arecibo detection of this burst had a significance of xxσ (Jason).

Figure **to do** shows the dynamic spectrum formed from the phased VLA and Arecibo data... **Discuss dispersion correction, time alignment, chance of false association**

This simultaneous detection of a burst from roughly 1 to 4 GHz shows that some bursts cover more than an octave of frequency. However, this is one of three VLA bursts with coverage by Arecibo, so the other nondetections imply that those bursts had a smaller spectral width. In fact, as described in §3.2.1, many of the VLA bursts appear to be fully contained in the band from 2.5 to 3.5 GHz, which implies a much smaller spectral coverage for typical bursts.

3.2. *VLA Bursts*

3.2.1. *Spectra*

Figure 2 shows the dynamic spectra of all nine bursts detected by the VLA. We improved on the initial analysis presented in Chatterjee et al (2017) by using a better calibration scheme and optimizing the detection significance over a find grid of DM ($\Delta DM = 1$pccm^{-3}). Table 1 shows the improved burst parameters using this new scheme.

Figure 3 shows the spectrum of the integration and DM that maximizes the burst detection significance. After DM optimization, all bursts appear unresolved at the 5 ms time resolution of the VLA data. One possible exception is the brightest burst at 57633.68, for which roughly 10% of the peak flux density is seen in adjacent 5 ms integrations.

The burst spectra are generally characterized by a broad, Gaussian shape that with strong inter-channel modulation. We fit a Gaussian shape to each burst to estimate their characteristic width and peak flux, as summarized in Table 1. The channel-scale modulation is as high as 100% (see §3.2.3) and is consistent with an exponential distribution. This introduces a strong bias to the best-fit Gaussian, but these simple fits are reliable enough to show that the typical burst has a spectral width of 500 MHz.

All but two of the best-fit Gaussians are centered inside the 3 GHz band and most appear contained by the 1 GHz wide band. This is consistent with previous detections of FRB 121102by Arecibo, which showed quasi-

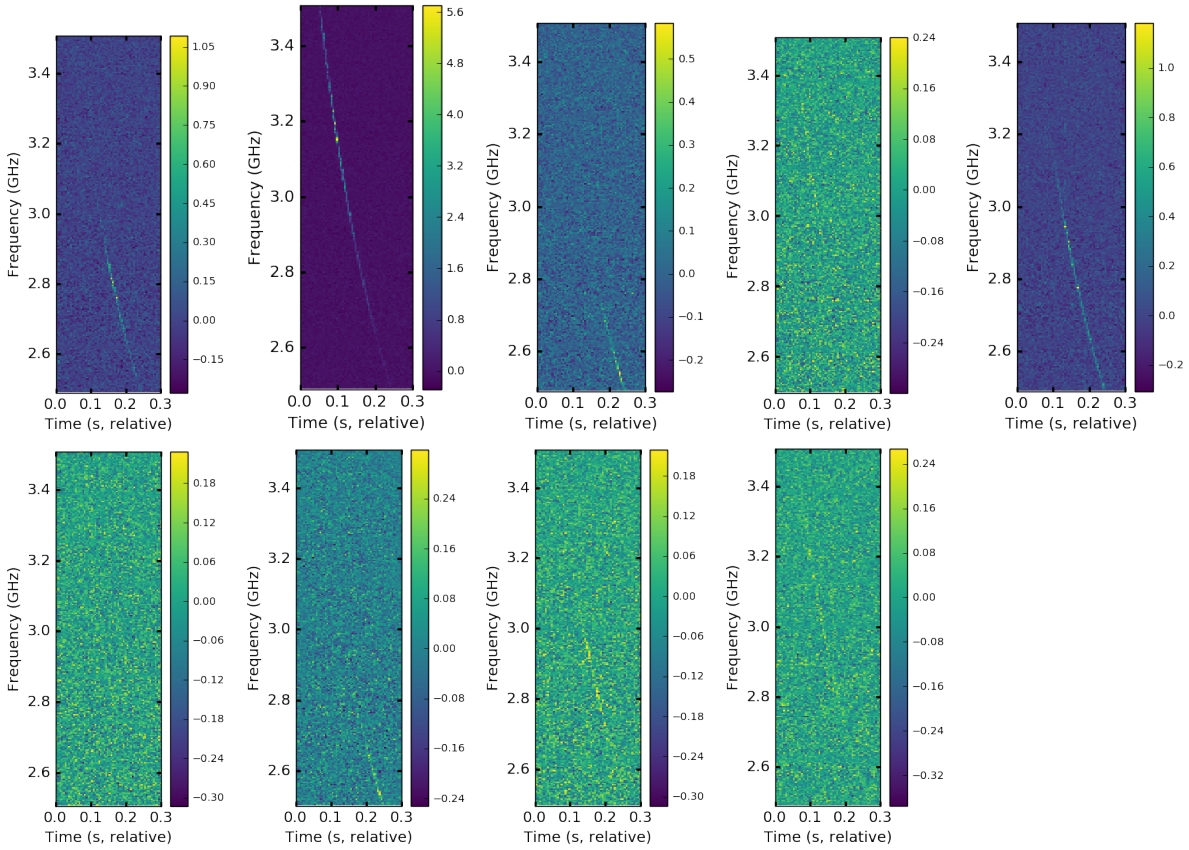

Figure 2. Dynamic spectra (time vs frequency intensity maps) for the nine VLA bursts. Starting at the top left, they correspond to bursts 57623, 57633.68, 57633.70, 57638, 57643, 57645, 57646, 57648, and 57649. Note that bursts are detected in 5 ms images generated from dedispersed visibilities.

broadband structure (Scholz et al. 2016) and large variation in the implied spectral index (Spitler et al. 2014). A detailed discussion of high-resolution FRB 121102 burst spectra seen by the Arecibo Observatory will be presented elsewhere (Hessels et al 2017).

3.2.2. *Dispersion*

The initial VLA detections were made by searching a DM grid that allowed inter-DM sensitivity losses up to roughly 10% ($\Delta DM = 10 \mathrm{pccm}^{-3}$ Cordes & McLaughlin 2003). In optimizing detection significance over a fine DM grid, we find optimal DM values range from 552 to 572 pc cm^{-3}. However, the uncertainty in the peak DM measurement is defined by the DM sensitivity loss curve and the significance of the burst.

Given that the apparent DM can potentially change due to intrinsic or extrinsic effects, we developed a more sophisticated system for modeling dispersion. We created a generative model to sample the likelihood distribution of a class of dispersion models (Hogg et al. 2010). We use the Gaussian shape (see §3.2.1) along the spectral axis and apply a frequency-depndent delay for a given dispersion model. The likelihood is directly sampled by calculating the product of probabilities on a per-pixel basis of the 2-dimensional dynamic spectrum. Uncertainties in each pixel are drawn from a uniform Gaussian error distribution that is estimated from the data.

Figure 4 compares the 95% confidence intervals on the DM for all nine VLA bursts. Some of the confidence intervals do not overlap, which suggests that there are apparent DM changes between bursts. This change could be caused by intrinsic burst structure (Hessels et al 2017) or actual changes to the DM column density. **Preliminary**

3.2.3. *Spectral Autocorrelation*

Autocorrelation of the burst signal (both temporal and spectral) can be used to infer both intrinsic properties and modulation due to scintillation (CITE: Cordes et al?). While VLA spectral resolution of 4 MHz is relatively coarse, diffractive scintillation observed for other FRBs () could/could not (Jim?) induce structure on this scale near 3 GHz.

Figure 5 shows the spectral autocorrellation for the strongest burst (MJD 57633.68). Comment, Jim?

Table 1. Properties of Bursts from FRB 121102

Date (MJD)	S_{int} (mJy)	Image SNR	L_{int} (10^{38} erg)	DM_{opt} (pc cm^{-3})	S_{peak} (Jy)	Center (GHz)	FWHM (MHz)
57623	258	38	15	561	0.41	2.8	300
57633.68	2000	179	120	554	1.90	3.2	520
57633.70[a]	105	15	6	559	>0.188	<2.5	>350
57638	65	12	4	556	0.07	3.1	410
57643	375	100	21	560	0.39	2.8	520
57645	38	13	2	572	0.06	2.8	210
57646[a]	69	20	4	555	>0.16	<2.5	>400
57648[b]	97	25	6	559	0.11	2.9	420
57649	110	36	6	552	0.07	2.9	880

[a] Best-fit Gaussian is not centered in 3 GHz band, so spectral parameters are limits.

[b] Detected simultaneously with Arecibo between 1.15 and 1.73 GHz.

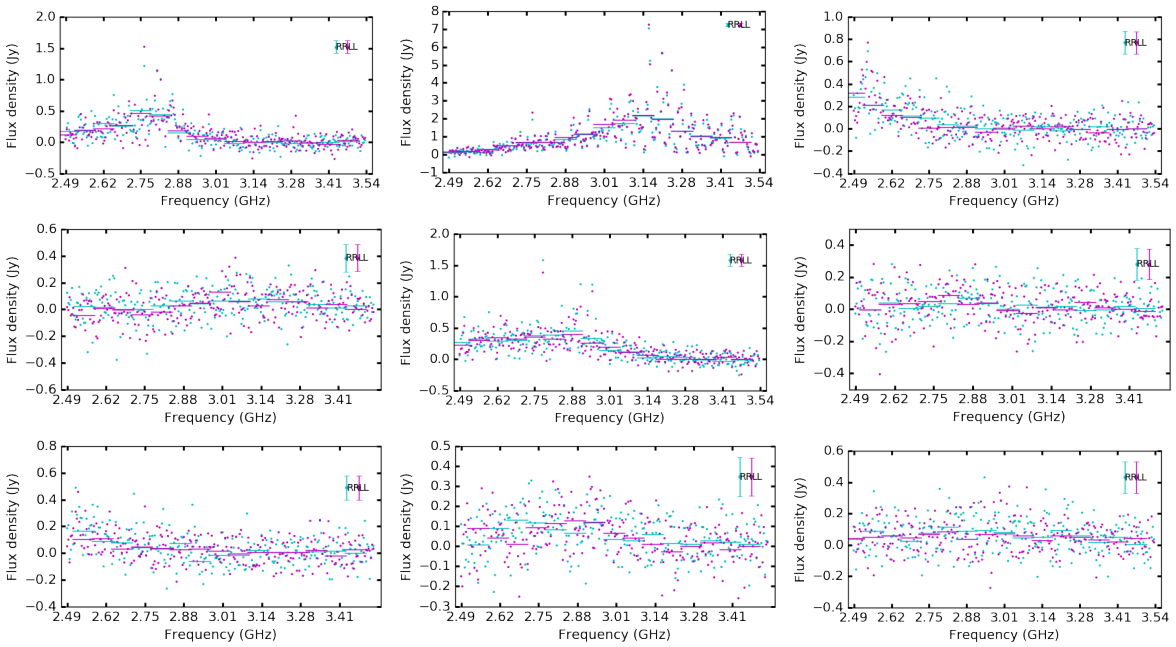

Figure 3. Spectra of nine bursts seen by the VLA from 2.5 to 3.5 GHz. Orthongonal circular polarizations (RR and LL) are plotted separately. **LABELS ALL SAME FREQ. SOME SHOULD START HIGHER FOR DROPPED CHANNELS**

3.2.4. *Circular Polarization*

The VLA S-band recievers natively measure circular polarization, although for observing efficiency we chose not include polarization calibration procedures. Crude constraints on circular polarization are possible by comparing the burst intensity in right and left-hand polarized data products. The apparent circular polarization fraction $((RR-LL)/(RR+LL))$ for the most significant bursts are all less than 3%. FRB 121102was located 2.3 arcmin away from pointing center, where systematic effects have been measured as large as 3% (Perley et al 2016, VLA memo). Given that systematic effects dominate the apparent circular polarization, we conclude that the true fractional circular polarization is less than 3%.

3.3. *Temporal Statistics*

The VLA detected nine bursts during the month-long campaign in August–September 2016. The typical observation lasted about two hours and was sampled with a 5 ms cadence, so we used the Lomb-Scargle periodogram

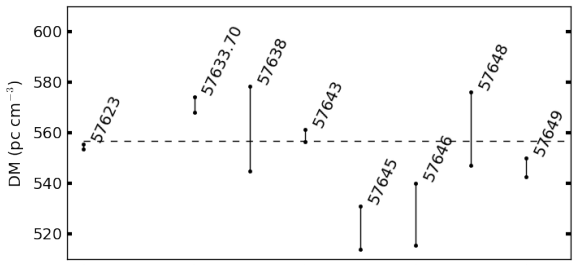

Figure 4. **Preliminary** Comparison of 95% (1*sigma*) confidence intervals for DM for nine bursts detected by the VLA.

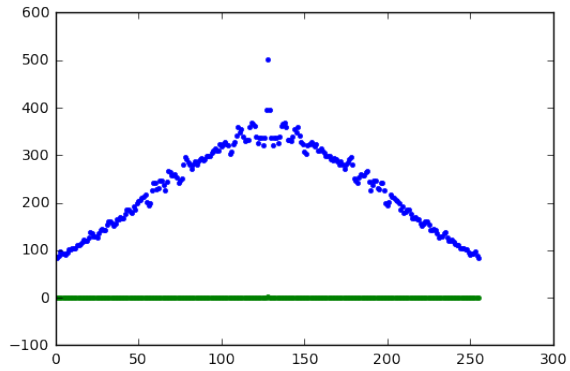

Figure 5. The spectral autocorrelation for the burst from FRB 121102 at MJD 57633.68. Blue shows the autocorrelation for the burst and green shows an autocorrelation of a representative spectrum with no burst.

() to search for periodic structure over a wide range of timescales. The input "lightcurve" was mde as a one-dimensional array for all times with observations; times with a detection are set to 1 and other times are set to 0 (Palliyaguru et al. 2011, see also). The lightcurve time resolution was set to 100 ms (check) to keep the computation manageable. The 95% confidence upper limit on periodic power is estimated by randomly selecting the 9 burst times from the same observing times. The limit is set as the 95% highest point at each period (5th highest value in 100 simulations).

Figure 6 shows the Lomb-Scargle periodogram for the bursts for periods from **xx to xx** s. No significant excess power is seen at long periods, but the periodogram shows a steady increase in power at shorter periods. The periodogram exceeds the 95% power limit for periods from xx to xx s (**limited by binning time?**). This is consistent with the idea that the bursts imperfectly trace an underlying rotational period, as has been observed from many classes of neutron star. Examples include magnetars, which typically have wide pulse phase windows (), pulsars with glitches that change their periods (), and Maura? also refs for previous points would be welcome. However, we can show with simulations that nine bursts drawn from a simple rotational would produce a strong, narrow peak in 6.

Assuming periods with power peaks, we find clusters of bursts with same rotational phase...

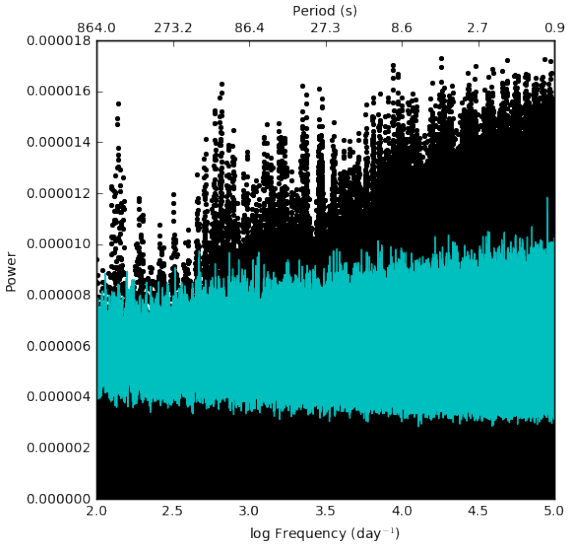

Figure 6. Dots show the Lomb-Scargle periodogram of burst arrival times for FRB 121102. The solid line show the 95% confidence upper limit on the power expected from bursts with random arrival times. (**New version being compiled**)

Burst detections were made very inhomogenously through the larger (63 hours) observing campaign of FRB 121102. In the first 30 hours of observing at S-band no bursts were detected, while nine bursts were detected in the last 27 hours of S-band observing. The data quality is high and RFI did not significantly impact sensitivity, so the inhomogeneous burst distribution shows that the burst detection probability was not stationary. Assuming that the burst detection probability follows a Poisson distribution, the nondetection in the first half of S-band limits the FRB rate to R < 0.1 hour^{-1} (95% confidence limit). The mean detection rate for the last part of the campaign was R $= 0.3$ hour^{-1}.

Moreover, there is weak evidence that the FRB 121102 burst rate changes during the last part of the campaign. We modeled the event detection probability as a Poisson probability with a rate parameter that evolves linearly with time relative to first burst detection. We directly sampled the model by calculating the joint probability $\prod_i P_i$, where P_i follows a Poisson probability with rate $\lambda = a + b * (\mathrm{MJD_i} - 57623)$. Figure 7 shows that the

probability distribution excludes a constant rate with ∼85% confidence. This weak constraint is consistent with the broader trend seen by the VLA and Arecibo (Hessels et al 2017).

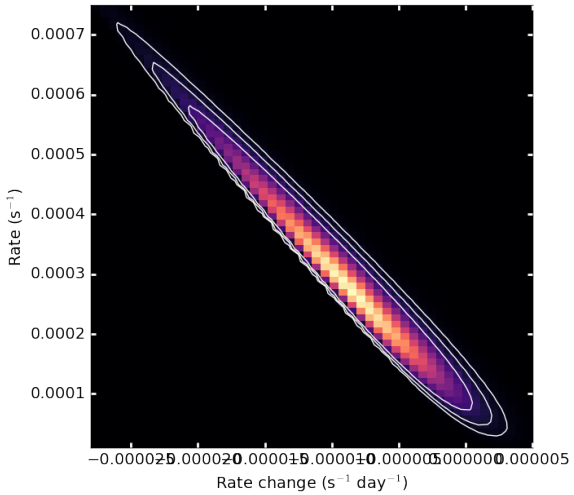

Figure 7. Color scale and contours show the relative probability for a time-evolving Poisson detection probability for FRB 121102. Contours show the 50, 90, and 95% confidence contours on the rate a (bursts s^{-1}) and rate change b (bursts s^{-1} day^{-1}) during the August–September 2016 campaign in which bursts were detected.

3.4. *Brightness Distribution*

Knowing the burst distance, we calculate their mean luminosity across a single 5 ms integration and the 1 GHz bandwidth (Table 1). The VLA has also shown for the first time that most bursts are contained within the 3 GHz band. That means that the mean S-band flux density can be converted to a luminosity in units of ergs with no assumptions about its spectral properties.

With a uniform sample of burst luminosities, we can use their distribution to infer more general properties for FRB 121102. Figure 8 shows the luminosity distribution of the VLA bursts with a best-fit powerlaw model. Fitting a powerlaw model to the cumulative luminosity distribution gives an index of –0.5. The flatness of the distribution is also clear from range of significance of the nine bursts (12 to 179σ). All bursts are much brighter than the sensitivity limit (weakest is $\sim 10\sigma$), so the distribution is not affected by a completeness limit.

4. DISCUSSION

4.1. *Emission Physics and Burst Energetics*

Cut from gemini paper The redshift measurement allows us to put FRB 121102's energetics on a firmer footing, confirming Chatterjee et al (2017).

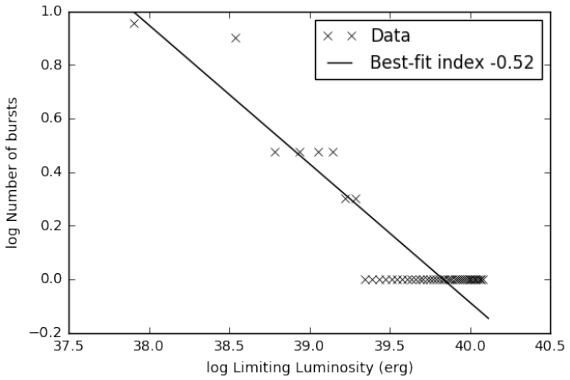

Figure 8. Cumulative luminosity distribution and best-fit powerlaw model for the nine VLA bursts from FRB 121102.

For a nominal Gpc distance D corresponding to redshifts $z \lesssim 0.3$, the received fluence A_ν from each burst implies a burst energy

$$E_{\rm burst} = 4\pi D^2 (\delta\Omega/4\pi) A_\nu \Delta\nu \approx 10^{38}\,{\rm erg}\,(\delta\Omega/4\pi) D^2_{\rm Gpc} (A_\nu/0.1\,{\rm Jy\ m}$$

The unknown emission solid angle $\delta\Omega$ could be very small due to relativistic beaming, and together with a distance possibly much smaller than 1 Gpc, could reduce the energy requirement significantly. However, the *total* energy emitted could be larger depending on the duration of the emission in the source frame and other model-dependent details. Either way, the burst energies from FRB 121102 are not inconsistent with those that might be expected from the magnetosphere of a compact objectCordes & Wasserman (2016).

4.2. *Luminosity Distribution*

Doubts were cast on the first FRB detection ("Lorimer burst") due to its unusually high brightness. The lack of lower-significance detections suggested that this burst was unlikely to be part of any astrophysical population. With more detections, it has become clear that the FRB population has a relatively flat flux distribution (Vedantham et al. 2016; Lawrence et al. 2016). This fact was demonstrated with yet another detection of an extremely bright FRB (Ravi et al. 2016).

FRB 121102 is detectable with the VLA out to $z = 0.7$ and much farther with Arecibo...

Discuss comparison FRB 121102 luminosity distribution to that of FRB population...

Imagine physical log N/log S with cut-offs and scattering can bias the intrinsic into the observed distribution (Macquart and Johnston)...

Simulate cosmic volume uniformly filled with FRB 121102... Also once done with a theoretical model based on young pulsars (Lyutikov et al. 2016)

Scaling up assumes that this source is representative. Propagation effects may amplify or alter burst brightness statistical properties. Some such effects are possible near the burst source (e.g., Jim's caustic analysis), which would effectively be intrinsid in this context.

4.3. *Repetition*

Discussion of "red spectrum" and Connor et al. (2016). Bursts predict bursts therefore repetition constraints of other FRBs are likely weaker than claimed...

Constraints on repetition assuming "red spectrum" for whole population. Simulation using observed burst temporal statistics...

Intrinsic versus refractive scintillation...

Fewer FRBs out there...

4.4. *FRB Rate*

Assuming that FRB 121102is from the same population as the other FRBs, the measurement of a distance for the host of FRB 121102allows us to re-evaluate the cosmic volume and event rate per galaxy for the FRB population. The estimated projected FRB rate R_p understates the true rate by a beaming fraction Ω_b ($\sim$10%; Tauris & Manchester 1998).. For a comoving volume $V(z)$ and galaxy number density $\Phi(M)$, the rate per galaxy is $R_{FRB} = R_p\Omega_b/(\Phi(M)V(z))$.

The first such rate estimate was made by Thornton et al. (2013), who used the measured DM to estimate a characteristic distance for their sample of 4 FRBs. They assumed that all of the extragalactic component of the DM was caused by the IGM and scaled as $DM \approx z \times 1200\mathrm{pccm}^{-3}$ (Ioka 2003; Inoue 2004). They also calculated the number of galaxies by assuming a characteristic L_* galaxy (corresponding to stellar mass $M_* \approx 1010.66M$ Baldry et al. 2012).

Our calculation differs in that we have better estimates of all three parameters. First, the projected FRB rate is now believed to be closer to $2 \times 10^3\mathrm{sky}^{-1}\mathrm{day}^{-1}$ at high Galactic latitudes and flux densities brighter than 1 Jy ms (Lawrence et al. 2016; Champion et al. 2016). FRB 121102 is associated with a relatively small galaxy, which are roughly a factor of 100 more abundant ($\Phi(M) \approx 10^{-2}\mathrm{Mpc}^{-3}$ Faber et al. 2007). Finally, the measured distance for FRB 121102 suggests that roughly half of the extragalactic DM is intrinsic to the host and half is from the IGM.

This reduces the characteristic distance by a factor of two and the volume by an order of magnitude. Considering these factors, we assume a characteristic FRB redshift of 0.4 to estimate $R_{FRB} \approx 10^{-4}(0.1/\Omega_b)\mathrm{galaxy}^{-1}\mathrm{year}^{-1}$, which is two orders of magnitude lower than previously estimated (Thornton et al. 2013, assuming isotropic radiation;).

There are significant caveats to the comparison of this rate to the rates of other classes of transient. This isotropic FRB rate assumes a projected FRB rate at a single (observationally defined) flux limit and that no bursts repeat. Using this calculation with data from more sensitive telescopes, we might infer a higher rate. However, if we assume that FRB 121102 is representative of the overall FRB population, then more sensitive observations would be more likely to find repeating FRBs that would effectively depress the estimate of the underlying isotropic rate per source. In this model, these two effects partially cancel, although without a physical model it is difficult to say how well.

4.5. *Observing Strategies*

Repetition implies that targeting known FRBs is optimal.

Repetition and shallow luminosity distribution show that shallow and wide is the best way to blindly find FRBs.

Given that bursts have < 1 GHz-scale spectra, wide bandwidths improve odds of detection.

4.6. *Naming Convention*

The cosmological distance for FRB 121102 and consistency with the overall population suggests that most FRBs repeat. The current naming convention for FRBs is analogous to supernovae, with six numbers defining the year, month, and day of detection. If all FRBs repeat, then this naming convention is only useful for identifying its discovery. A more useful convention would be the more common one that uses the coordinates. But there are already two FRBs that have consistent celestial positions and different DMs.

We suggest a convention of referring to FRBs as Jhhmm+dd or appending DM...

5. CONCLUSIONS

ACKNOWLEDGEMENTS

We thank ... This project was supported by the University of California Office of the President under Lab Fees Research Program Award 237863. The National Radio Astronomy Observatory is a facility of the National Science Foundation operated under cooperative agreement by Associated Universities, Inc.. This research made use of Astropy, a community-developed core Python package for Astronomy (Astropy Collaboration, 2013).

REFERENCES

Baldry, I. K., et al. 2012, MNRAS, 421, 621

Champion, D. J., et al. 2016, MNRAS, 460, L30

Chatterjee et al. 2017, Nature

Connor, L., Pen, U.-L., & Oppermann, N. 2016, MNRAS, 458, L89

Cordes, J. M., & McLaughlin, M. A. 2003, ApJ, 596, 1142

Cordes, J. M., & Wasserman, I. 2016, MNRAS, 457, 232

Faber, S. M., et al. 2007, ApJ, 665, 265

Falcke, H., & Rezzolla, L. 2014, A&A, 562, A137

Hessels et al. 2017, in prep

Hogg, D. W., Bovy, J., & Lang, D. 2010, ArXiv e-prints

Inoue, S. 2004, MNRAS, 348, 999

Ioka, K. 2003, ApJL, 598, L79

Katz, J. I. 2014, PhRvD, 89, 103009

—. 2016, Modern Physics Letters A, 31, 1630013

Law, C. J., et al. 2015, ApJ, 807, 16

Lawrence, E., Vander Wiel, S., Law, C. J., Burke Spolaor, S., & Bower, G. C. 2016, ArXiv e-prints

Lorimer, D. R., Bailes, M., McLaughlin, M. A., Narkevic, D. J., & Crawford, F. 2007, Science, 318, 777

Luan, J., & Goldreich, P. 2014, ApJL, 785, L26

Lyutikov, M., Burzawa, L., & Popov, S. B. 2016, MNRAS, 462, 941

Macquart, J.-P., & Johnston, S. 2015, MNRAS, 451, 3278

Marcote et al. 2017, ApJL

McQuinn, M. 2014, ApJL, 780, L33

Palliyaguru, N. T., et al. 2011, MNRAS, 417, 1871

Perrott, Y. C., et al. 2013, MNRAS, 429, 3330

Petroff, E., et al. 2015, MNRAS, 454, 457

Planck Collaboration et al. 2016, A&A, 594, A13

Ravi, V., et al. 2016, ArXiv e-prints

Scholz, P., et al. 2016, ArXiv e-prints

Spitler, L. G., et al. 2014, ApJ, 790, 101

—. 2016, Nature, 531, 202

Tauris, T. M., & Manchester, R. N. 1998, MNRAS, 298, 625

Tendulkar et al. 2017, ApJL

Thornton, D., et al. 2013, Science, 341, 53

Vedantham, H. K., Ravi, V., Hallinan, G., & Shannon, R. M. 2016, ApJ, 830, 75